Colloids and Surfaces B: Biointerfaces 89 (2012) 108–116

Contents lists available at SciVerse ScienceDirect

Colloids and Surfaces B: Biointerfaces

journal homepage: www.elsevier.com/locate/colsurfb

Synthesis of mesostructured polyaniline using mixed surfactants, anionic sodium dodecylsulfate and non-ionic polymers and their applications in H_2O_2 and glucose sensing

M.U. Anu Prathap[a], Bhawana Thakur[b], Shilpa N. Sawant[b,1], Rajendra Srivastava[a,*]

[a] Department of Chemistry, Indian Institute of Technology Ropar, Rupnagar, India
[b] Chemistry Division, Bhabha Atomic Research Centre, Mumbai, India

ARTICLE INFO

Article history:
Received 21 July 2011
Received in revised form 1 September 2011
Accepted 4 September 2011
Available online 10 September 2011

Keywords:
Mesoporous material
Polyaniline
Structure directing agents
Glucose biosensor
Electrochemical detection

ABSTRACT

Mesostructured polyaniline was prepared by the self-assembly of a mixture of an anionic surfactant, sodium dodecylsulfate and a non-ionic polymeric surfactant (polyethylene glycol, and block-co-polymers such as Pluronic P123 and Brij-35). Materials were characterized by a complementary combination of X-ray diffraction, Scanning electron microscopy, Fourier-transform infrared spectrometer and UV-visible spectrophotometer. Mesostructured polyaniline was used for construction of biosensor, which displayed excellent electrocatalytic response for the detection of H_2O_2 and glucose compared to conventional polyaniline. The electrocatalytic response observed in the case of mesostructured polyaniline can be correlated with the large surface area and nanopores which enhances the accessibility of H_2O_2/glucose molecule to the active site that result in high observed current. The methodology adopted in the present study provides a new platform for the fabrication of polyaniline based high-performance glucose and other biosensors.

1. Introduction

Organic porous materials are a class of advanced materials which possess enormous potential for many technological applications [1]. Conducting polymers are novel porous organic semiconducting materials which have attracted considerable attention because of their remarkable optical, electrochemical, and conducting properties [2]. In recent years, there has been increased interest in the synthesis of one-dimensional nanostructures of conjugated polymers, because they possess astonishing physical and chemical properties. Among various conducting polymers, polyaniline (PANI) has attracted significant attention because it exhibits remarkable environmental stability and its electrical properties can be tuned by varying the oxidation state and protonation state [3,4]. Nanostructured polyaniline combines the properties of low-dimensional organic conductors with high surface area materials. Nanostructured polyaniline materials find applications in gas-separation membranes [5], polymeric conducting molecular wires [6], light emitting and electronic devices [7], chemical sensors [8], electrorheological material [9], biosensors, vapour sensing applications [10,11], and neuron devices [12]. A variety of synthesis approaches Such as seeding polymerization [13], hard template method [14], soft template method [15,16], interfacial polymerization [17], electrospinning [18], and ultrasonic irradiation [19] have been developed for the synthesis of PANI nanostructures. It may be noted that pure PANI nanofibers/tubes and spheres can be obtained even in the absence of any templates or external physical routes [20,21]. However, this method requires large organic acids that serve as both, dopants and in situ templates by forming micelles upon which aniline is polymerized but fiber diameters are highly influenced by reagent ratios [20]. Uniform PANI nanofibers were also prepared by using interfacial polymerization approach, at an aqueous–organic interface [17,21]. In this method aniline was co-dissolved in the organic phase, while ammonium peroxydisulfate (APS) in aqueous acidic phase, giving rise to the films at the interface of the two immiscible liquids. Please note that using interfacial polymerization approach, the yield of PANI nanofibers was very low [21] and this method required organic solvents to dissolve an aniline monomer and produced a waste stream that should be processed separately. Electrochemical polymerization [22] and some physical methods, such as electrospinning [23] and mechanical stretching [24] can also produce PANI nanomaterials, but these materials have only been made on a very limited scale, such as films on an electrode surface. Generally, the template synthesis method (hard template or soft template) is considered to be the most effective route to prepare micro/nano-structure conducting

* Corresponding author. Tel.: +91 1881 242175; fax: +91 1881 223395.
E-mail addresses: stawde@barc.gov.in (S.N. Sawant), rajendra@iitrpr.ac.in (R. Srivastava).
[1] Tel: +91 022 25590288.

0927-7765/$ – see front matter © 2011 Elsevier B.V. All rights reserved.
doi:10.1016/j.colsurfb.2011.09.002

polymers. When hard templates were used as a structure directing agent, the dimension of the resultant conducting polymers was governed by the porous network structure of hard templates [25]. Inorganic aluminum oxide [26], zeolite [6], and anodic aluminum oxide [25] were commonly used as the hard-templates. However, in hard template approach, the oriented structures of the resultant products generally disturbed while etching the template from the materials (the use of harsh chemicals, strong acid/base or organic solvents). Soft template method uses organic surfactants, which guide the growth of polymer or act as a structure directing agent. Soft-templates can be easily removed from the final product, just by controlled calcinations or by mild acidic/basic washing. PANI synthesized using organic surfactant possesses high surface area [27]. PANI having high surface area offer many advantages such as good thermal, chemical, and mechanical stability as well as an excellent enzyme entrapment matrix for biosensing application [28,29]. The efficient method to enhance the surface area of nanostructured PANI is to induce mesophase by using surfactant, which forms supramolecular assembly [30]. Use of mixed surfactant/co-surfactant system has been known as a better method to control the size and shape of the nanoparticles over single surfactant [31]. The particle growth in a mixed surfactant/co-surfactant system is quite complicated, which directly influences the particle size and surface functionality.

The determination of glucose and H_2O_2 concentrations is important in several aspects for food, microorganism or medicine [32–34]. The development of a glucose biosensor is important due to the prevalence of cardiovascular diseases as a major health threat around the world [35]. Several approaches are known to detect glucose and similar biomolecules. These include surface plasmon resonance biosensor, near-infrared optical biosensor, capacitive detection, electrochemiluminescene, fluorescence detection, colorimetry, and amperometric biosensor, etc. [36]. Among all methods, amperometric glucose biosensor is a promising method since it has the advantages of high sensitivity, compatibility for miniaturization, easy operation, and low cost. Nanomaterials provide high surface areas for higher enzyme loading and a compatible microenvironment helping the enzyme to retain its bioactivity [37]. Besides this, they provide direct electron transfer between the enzyme's active site and the electrodes [38,39].

Herein, we report a novel method to synthesize mesostructured PANI by using the self-assembly of a mixture of an anionic surfactant sodium dodecylsulfate (SDS) and a non-ionic polymeric surfactant [tri-block co-polymer, poly(ethylene glycol)-*block*-poly(propylene glycol)-*block*-poly(ethylene glycol) ($EO_{20}PO_{70}EO_{20}$) (hereafter written as P123), polyoxyethylene lauryl ether (hereafter written as Brij-35), and polyethylene glycol-4000 (hereafter written as PEG)] as a structure directing agent (SDA). The mesostructured PANI is further used for the construction of biosensor, which displayed excellent electrocatalytic response for the detection of H_2O_2 and glucose compared to conventional PANI. To the best of our knowledge, such improved sensitivity and linear range for detection of glucose and H_2O_2 molecules with mesostructured PANI is reported here for the first time.

2. Materials and methods

2.1. Materials

All chemicals used in the study were of A.R. grade. Aniline was vacuum distilled and stored in the dark. Aniline, hydrogen peroxide (30%), ammonium peroxydisulphate (APS), HCl and sodium dodecylsulfate (SDS) were obtained from Merk India Pvt. Ltd. $HO(CH_2CH_2O)_{20}(CH_2CH(CH_3)O)_{70}(CH_2CH_2O)_{20}H$ ($EO_{20}PO_{70}EO_{20}$), MW = 5800, designated Pluronic P-123, polyethylene glycol (PEG, MW = 4000) and polyoxyethylene lauryl ether (designated Brij-35, MW = 1225) was obtained from Aldrich. Glucose oxidase (GOx, Type II-S from Aspergillus niger) was obtained from Sigma–Aldrich. Deionised water from Millipore Milli-Q system (Resistivity 18.2 MΩ/cm) was used in all cases to prepare aqueous solutions.

2.2. Methods

2.2.1. Sample preparation

Conventional PANI was prepared using the initial molar composition, 2.0 Aniline/2.0 HCl/4 APS, according to the reported procedures [40]. Then, PANI was prepared in the presence of only SDS as SDA. For this, first a dilute aqueous HCl was prepared (by mixing 1.7 g of commercially available 12 M HCl and 140 g water). Aniline (1.87 g) was dispersed in a dilute aqueous solution of HCl (40 ml) with magnetic stirring at room temperature for 0.5 h. This solution was added to an aqueous solution of SDS (2.88 g SDS and 100 ml dilute aqueous solution of HCl) under stirring condition to obtain a uniform mixture. The mixture was then placed in an ice-salt bath, so that the temperature was maintained at 277–278 K. Finally, ice cold aqueous APS (9.2 g APS and 100 ml water) was added slowly to the above mixture and the whole mass was allowed to become homogeneous. Then stirring was stopped and the mixture was allowed to age under the static condition for 2 days at 277–278 K. The molar ratio of the various constituents in the final reaction mixture was 2.0 Aniline/2.0 HCl/1.0 SDS/4 APS. Material prepared with SDS is designated as PANI-SDS.

PANI was also synthesized using mixed template method in which SDS was used as anionic SDA and polymeric template was used as non-ionic SDA. Materials were prepared using similar gel composition and synthesis method that was used for the synthesis of PANI using only SDS as SDA. Aniline (1.87 g) was dispersed in a dilute aqueous solution of HCl (40 ml) with magnetic stirring at room temperature for 0.5 h. This solution was added to an aqueous solution of SDA (1.5 g non-ionic polymers, 2.88 g SDS and 100 ml dilute aqueous solution of HCl) under stirring condition to obtain a uniform mixture. The mixture was then placed in an ice-salt bath, so that the temperature was maintained at 277–278 K. Finally, ice cold aqueous APS (9.2 g APS and 100 ml water) was added slowly to the above mixture and the whole mass was allowed to become homogeneous. Then stirring was stopped and the mixture was allowed to age under the static condition for 2 days at 277–278 K. Materials prepared using SDS + P123, SDS + Brij-35, and SDS + PEG are designated as PANI-SDS-P123, PANI-SDS-BRIJ35, and PANI-SDS-PEG, respectively. For the comparative purpose, PANI was also prepared using only P123 by following the above method and molar composition. PANI synthesized using only P123 is designated as PANI-P123. All samples were extracted in an aqueous solution containing ammonium acetate to remove the surfactant. Finally, the product was washed with de-ionized water followed by methanol until the filtrate became colorless. Product was dried in the oven at 60 °C for 24 h.

2.2.2. Material characterizations

X-ray diffraction (XRD) patterns were recorded in the 2θ range of 5–50° with a scan speed of 2°/min on a PANalytical X'PERT PRO diffractometer using Cu Kα radiation (λ = 0.1542 nm, 40 kV, 20 mA). XRD was also recorded in the low angle region in the 2θ range of 0.5–5°. Scanning electron microscopy (SEM) measurements were carried out on a JEOL JSM-6610LV, to investigate the morphology. Fourier-transform infrared spectrometer (FT-IR) spectra of the polymers were taken on a spectrophotometer model Bruker TENSOR-27 in the wave number range 400–4000 cm^{-1} (spectral resolution = 4 cm^{-1}; number of scans = 100). UV–visible spectra were recorded on Analytikjena Specord 250 PLUS

spectrophotometer with the PANI dispersed in deionized water as well as by dissolving in NMP in the wavelength range of 200–1100 nm (slit = 1 nm, scan speed 20 nm/s). Nitrogen adsorption measurement at 77 K was performed by Autosorb-IQ Quantachrome Instruments volumetric adsorption analyzer. Samples were out-gassed at 423 K for 4 h in the degas port of the adsorption apparatus. The specific surface area was determined by BET method using the data points of P/P_0 in the range of about 0.05–0.3.

2.2.3. Conductivity measurement

Since the conductivity and electrochemical properties of PANI are highly dependent on the pH, PANI samples prepared were equilibrated in 1 M HCl. For this, 0.50 g of PANI sample was placed in 10 ml of 1 M HCl and was stirred for 12 h using a magnetic stirrer. The solid was filtered, washed with deionized water and dried in vacuum at 60 °C for 24 h. For conductivity measurements, sample (0.1 g) was pelletized using IR pellet maker and contact points were made using silver paste.

2.2.4. Electrode fabrication

Cyclic voltammetry (CV) and amperometric studies of PANI-SDS-P123, PANI-SDS-BRIJ35 and PANI samples were performed using Potentiostat-Galvanostat PGSTAT20 (Ecochemie, The Netherlands). A three-electrode electrochemical cell was employed with Ag/AgCl as the reference electrode (KCl salt bridge), Pt disc (2 mm diameter) as the working electrode and Pt foil as the counter electrode. 1.5 mg PANI sample was dissolved in 15 μL DMF to give a concentrated solution. 10 μL of this concentrated solution was placed carefully on the Pt disc electrode and allowed to dry.

2.2.5. Immobilization of GOx into the PANI electrode

For immobilization of enzyme, the PANI electrode was dipped in 1% glutaraldehyde solution for 15 min, followed by rinsing with buffer. The glutaraldehyde treated electrode was dipped in GOx (10 mg/ml in phosphate buffer) solution for 1 h. The enzyme immobilized electrode was rinsed with buffer and was dried. PANI/GOx and PANI-SDS-P123/GOx electrodes were used for glucose sensing.

2.2.6. Preparation of solution

Glucose stock solution was prepared and kept at room temperature for about 24 h for mutarotation. Phosphate buffer 0.1 M was prepared by mixing 36 ml of 0.2 M dibasic sodium phosphate Na_2HPO_4 with 14 ml of 0.2 M of monobasic sodium phosphate $NaH_2PO_4{\cdot}2H_2O$ then dilute to 100 ml with distilled H_2O to get pH = 7.2 (298 K).

3. Results and discussion

3.1. Physico-chemical characterization

Wide angle XRD patterns of various PANI samples agree well with the reported literature [41,42] (Fig. 1a). The peak centered at $2\theta = 20.5^\circ$ can be ascribed to periodicity parallel to the polymer chain, while the peak at $2\theta = 25.3^\circ$ is caused by the periodicity perpendicular to the polymer chain [41]. The result suggests that the pore walls of polymer samples are composed of polyaniline framework moieties. Conventional PANI, PANI-SDS, and PANI-P123 did not show any low-angle reflections. However, low-angle reflection was observed for PANI-SDS-P123, PANI-SDS-BRIJ35, and PANI-SDS-PEG (Fig. 1b). A very sharp low-angle peak at $2\theta = 2.45^\circ$ was observed for PANI-SDS-P123, whereas a broad low-angle reflection centered at $2\theta = 2.3^\circ$ was observed for PANI-SDS-BRIJ35 and PANI-SDS-PEG samples. Low-angle reflection confirmed the presence of the ordered mesostructure. A sharp low-angle peak for PANI-SDS-P123 confirmed the existence of the highly ordered mesostructured PANI which was synthesized by using SDS and P123. Although this ordering is also present in PANI-SDS-BRIJ35 and PANI-SDS-PEG samples, but they are less ordered when compared with PANI-SDS-P123. Based on the XRD analysis one can conclude that mesostructured PANI can be prepared only when, both, SDS and non-ionic polymeric templates were used for the synthesis of PANI. After the removal of the templates using aqueous ammonium acetate, low angle order did not disturb (figure not shown) for these samples. This result suggests that the mesostructure ordering of PANI-SDS-P123, PANI-SDS-BRIJ35, and PANI-SDS-PEG was not disturbed even after the removal of the surfactant.

Table 1
Surface area, total pore volume, and conductivity of PANI samples synthesized in this study.

Sample	S_{BET} (m^2/g)	Total pore volume (cm^3/g)	Conductivity ($S\,cm^{-1}$)
PANI	35.4	0.034	0.00352
PANI-P123	43.3	0.042	0.00361
PANI-SDS	40.5	0.039	0.00405
PANI-SDS-PEG	55.9	0.054	0.00652
PANI-SDS-P123	83.6	0.085	0.0258
PANI-SDS-BRIJ35	61.8	0.06	0.00879

Surface area and pore volume of PANI was calculated from the N_2 adsorption–desorption isotherm. PANI samples synthesized in this study exhibited type IV isotherm but with different hysteresis loops (Fig. 1c). Conventional PANI exhibited H4 hysteresis loop, which shows that the material contains both, micropores and mesopores (Fig. 1c). PANI synthesized using dual templates exhibited H3 hysteresis loop, which shows that materials are having non-rigid aggregates like particles and signify the presence of slit shape pores (Fig. 1c). Materials exhibited broad pore size (4–10 nm) distribution (Fig. 1d). The surface area and pore volume of PANI materials are summarized in Table 1. Conventional PANI has the minimum surface area (35.4 m^2/g) whereas PANI-SDS-P123 has the highest surface area (83.6 m^2/g). Different morphologies were obtained when materials were synthesized using different SDA (Fig. 2). An aggregated morphology was obtained for the conventional PANI, whereas PANI-SDS/PANI-SDS-PEG exhibited a cloud-like morphology (Fig. 2). A mixed morphology was obtained for PANI-P123, in which brick slab like morphology (>1 μm) along with small aggregated crystal morphology (<100 nm) was obtained (Fig. 2). Again, an aggregated morphology was obtained for PANI-SDS-BRIJ35 and PANI-SDS-P123. However, the average particle size of PANI-SDS-P123 was found to be less than 100 nm, which is smaller than the particle size of conventional PANI (>200 nm) (Fig. 2). The particle size of PANI-SDS-BRIJ35 was more than PANI-SDS-P123 but less than conventional PANI.

FT-IR spectra of conventional PANI and PANI samples prepared in this study resembles with each other (Fig. 3a). Samples show characteristic absorption bands at 1562, 1478, 1300, 1243, 1132, and 821 cm^{-1}. The characteristic peaks at 1562 cm^{-1} and 1478 cm^{-1} can be assigned to the stretching vibration of quinoid ring and benzenoid ring, respectively [43]. The peaks at 1300 cm^{-1} and 1243 cm^{-1} correspond to the C–N stretching vibration [44]. Peak at 1132 cm^{-1} corresponds to the acid doping level. Single broad band at 820 cm^{-1}, which falls in the range of 800–860 cm^{-1} is due to 1,4-di-substituted benzene moiety [45]. To investigate the influence on acid doping level using FT-IR, as synthesized PANI-SDS-P123 was dedoped using 1 M NH_4OH for 12 h (two times). FT-IR investigation of dedoped PANI-SDS-P123 reveals that the broad peak of PANI-SDS-P123 at 1132 cm^{-1} disappeared and two sharp peaks at 1165 and 1115 cm^{-1} were observed (Fig. 3b) [46]. The FT-IR spectrum

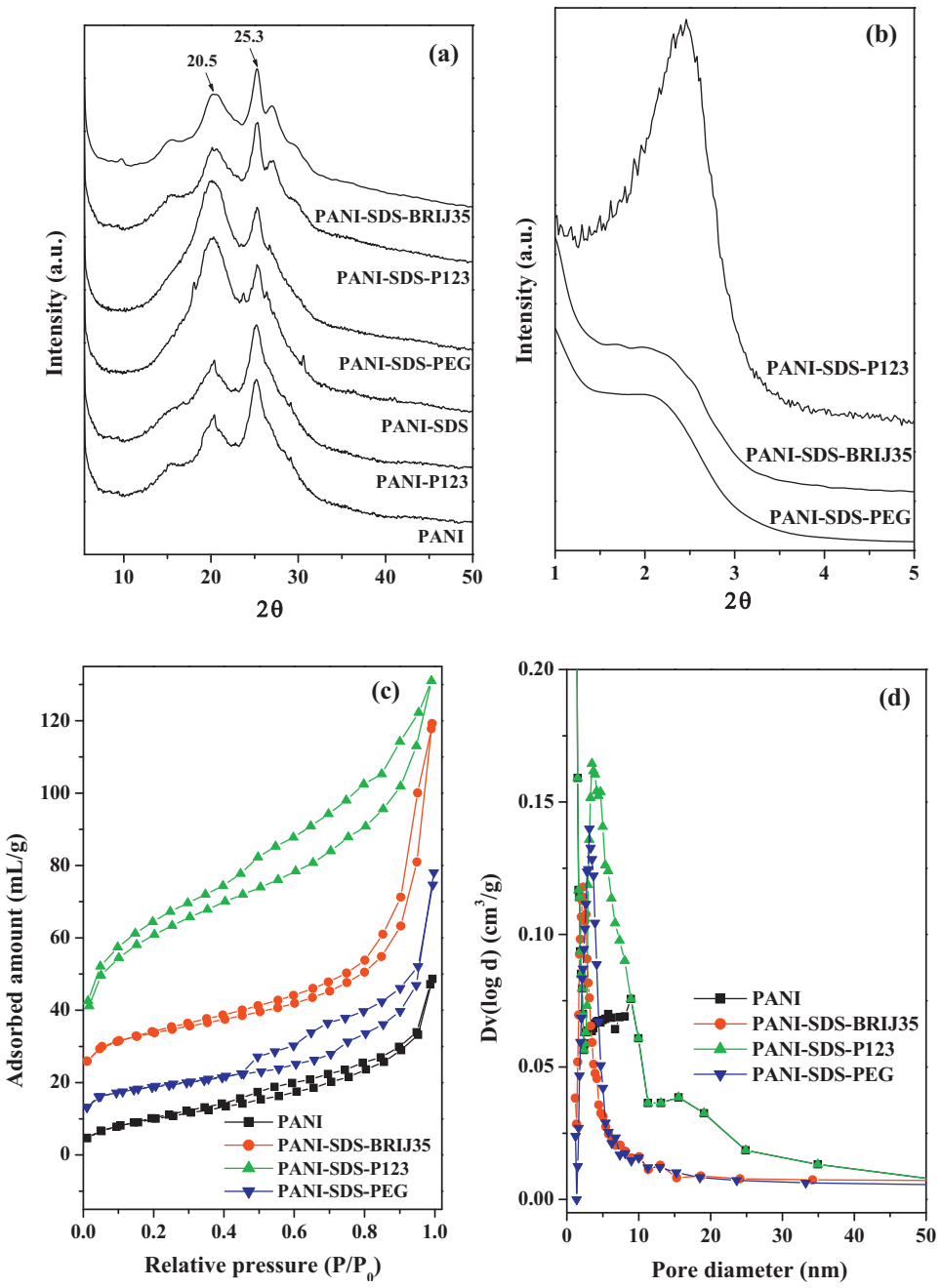

Fig. 1. (a) XRD patterns of PANI samples synthesized in this study, (b) Low-angle XRD patterns of PANI-SDS-P123, PANI-SDS-BRIJ35, and PANI-SDS-PEG. N_2 adsorption–desorption (c) isotherms and (d) pore size distributions of conventional PANI, PANI-SDS-P123, PANI-SDS-PEG and PANI-SDS-BRIJ35.

of PANI-SDS-P123 reveals that after dedoping the aromatic C–C stretching vibrations shift at 1562 cm^{-1} and 1478 cm^{-1} of as-synthesized emeraldine salt (ES) of PANI-SDS-P123 to 1589 cm^{-1} and 1500 cm^{-1} of emeraldine base (EB) of PANI-SDS-P123, respectively (Fig. 3b).

The UV–visible spectra of PANI were measured with samples dispersed in water [47,48] (Fig. 4a). Two peaks at 356 nm and 437 nm, which are assigned to the π–π^* benzenoid transition and the benzenoid to quinoid excitonic transition, respectively, were observed [49]. Besides these two peaks mentioned above, one additional peak λ_{max} = 741 nm for PANI & PANI-P123 and λ_{max} = 703 nm for PANI-SDS & PANI-PEG-SDS was also observed (Fig. 4a). Third peak represents the π-polaron transition, indicating that the materials are in the conductive state [50]. It may also be noted that PANI synthesized in the presence of SDS has an absorption at 283 nm which is present in all PANI samples, except PANI and PANI-P123 (Fig. 4a). Shifting of λ_{max} = 876 nm (from λ_{max} = 700–750 nm) for the materials PANI-SDS-P123 and PANI-SDS-BRIJ35 shows that the materials possess high conductivity [50]. For comparison, UV–visible spectra of PANI samples prepared in this study were taken by dissolving in NMP (Fig. 4b). Spectra obtained for these PANI samples in NMP, matched well with the reported spectra in literature [51]. To study the influence of dedoping on UV–visible spectrum, PANI-SDS-P123 was dedoped with 1 M NH_4OH solution for 12 h (twice). The UV–visible absorption spectra of dedoped PANI exhibit absorption bands with λ_{max} at 324 nm and 625 nm (Fig. 4c). The broad absorption at 625 nm for PANI has been assigned to quinoid formation in the backbone of the polymer [52] (Fig. 4c). The band around 324 nm is assigned to the π–π^* electronic transition of the benzene rings in the polymer backbone. Characteristic

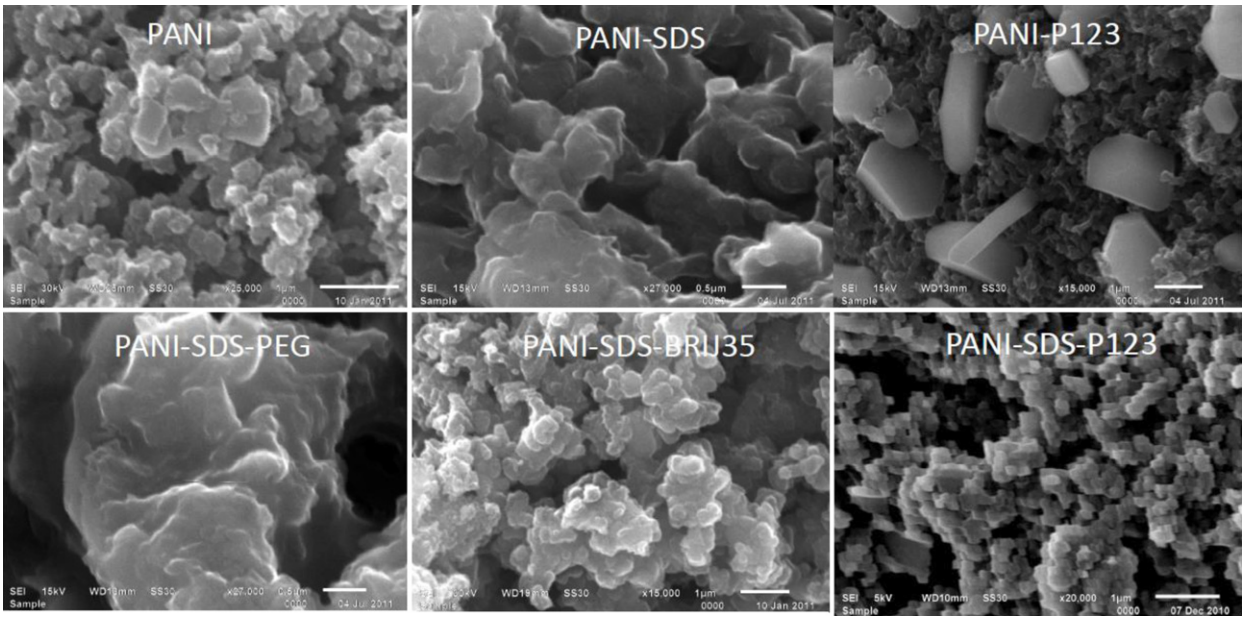

Fig. 2. SEM images of PANI samples synthesized in this study.

absorbance maxima in the as-synthesized PANI-SDS-P123 were observed at 437 nm and 876 nm due to the polaron band transitions in the polyaniline.

The conductivity of the PANI samples was measured by two-probe method. Room temperature conductivities of the pressed pellet of conventional PANI and template removed PANI samples prepared in this study are given in Table 1. Conductivity of PANI-SDS-P123 was found to be the highest among all the PANI samples. Since the conductivity of PANI-SDS-P123 was reasonably high, hence cyclic voltammogram for PANI-SDS-P123 was measured. For comparison, CV of PANI was also measured. PANI and PANI-SDS-P123 in 1 M HCl at the scan rate of 50 mV s^{-1} show that both samples have the typical reduction and oxidation responses of PANI (Fig. 5). It may be noted that, the PANI-SDS-P123 has a considerably high redox current and capacitance (Fig. 5), which indicates that more effective surface areas of the PANI-SDS-P123 is accessible to the electrolytes.

Neutral polymeric surfactants such as P123, Brij-35 and F127 are well known to prepare a variety of mesoporous materials [53,54]. In aqueous solution, hydrophilic PEO blocks and hydrophobic PPO blocks of P123 can self-assemble and form spheres, cylinders or bilayers on hydrophilic surface due to its amphiphilic nature in aqueous solution above a critical micelle concentration [53]. The basic structure of a P123 micelle consists of a well hydrated corona of PEO and a core of PPO blocks. When SDS is added, these micelles encapsulate SDS molecules in their cavity through hydrogen bonding. Upon introduction of hydrophobic aniline monomer, it will diffuse into the interior of micelle through hydrophobic–hydrophobic interaction. Consequently, when APS is

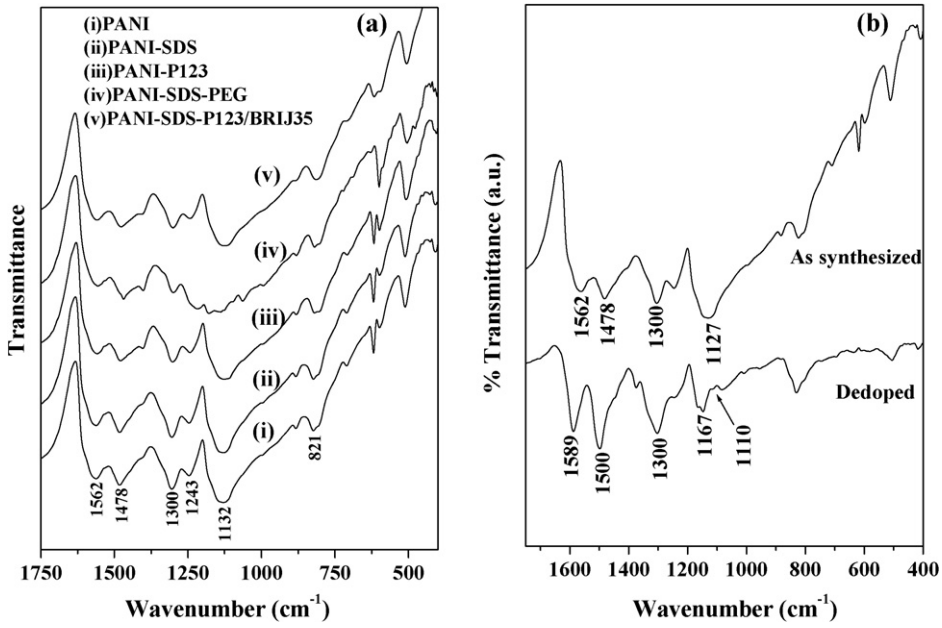

Fig. 3. FT-IR spectra of (a) PANI samples investigated in this study and (b) as-synthesized and dedoped PANI-SDS-P123.

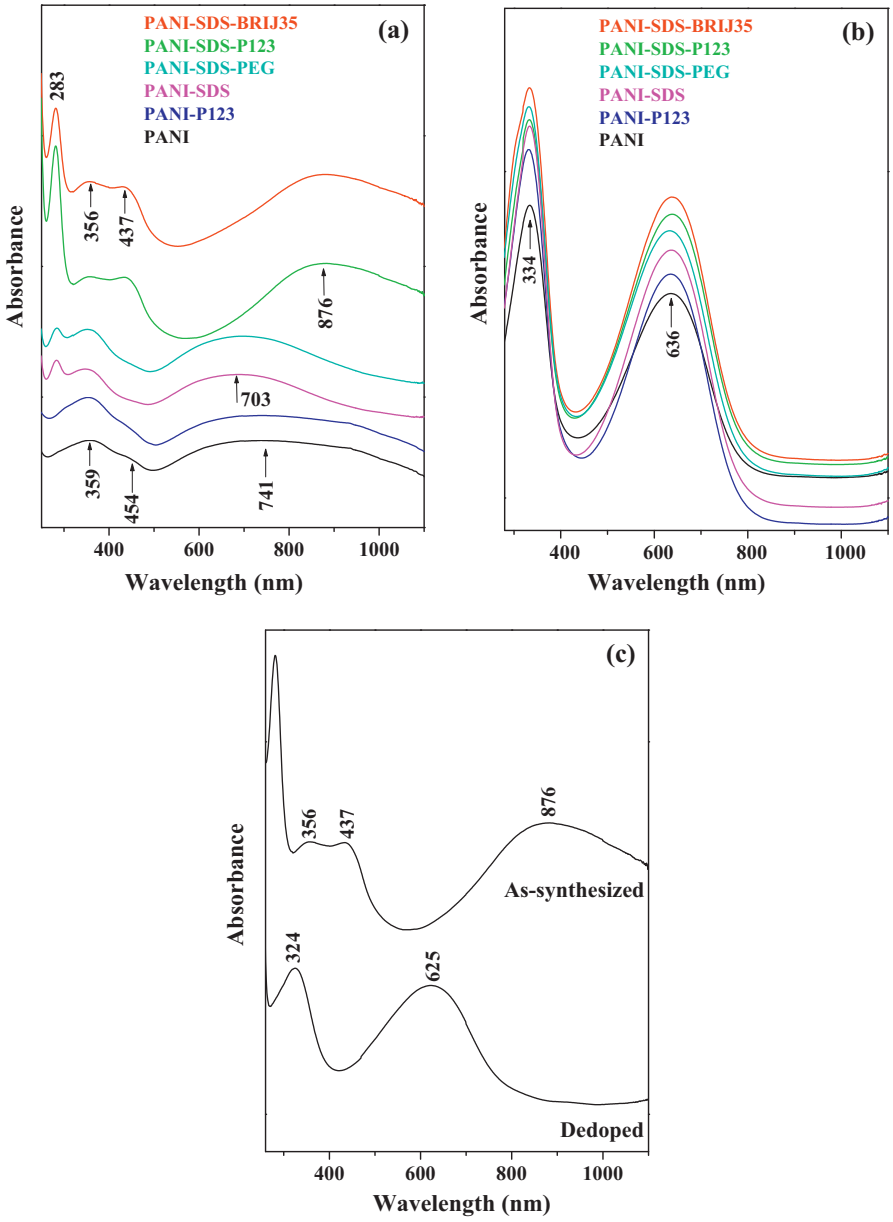

Fig. 4. UV–visible spectra of (a) PANI samples investigated in this study by dispersing in water. (b) PANI samples investigated in this study in NMP, and (c) as-synthesized and dedoped PANI-SDS-P123 by dispersing in water.

added to the reaction system, polymerization of aniline takes place resulting in uniform PANI layers. The idea behind taking mixed surfactant in our study is to organize these PANI frameworks to grow around its periphery through ionic interaction of the $C_{12}H_{25}SO_3^-$ and NH^+ moiety of growing PANI chain. Based on the experimental observations, a model has been proposed to represent ordered PANI mesostructure (Scheme 1a).

3.2. Electrochemical sensing of H_2O_2

H_2O_2 sensing was performed using CV and continuous amperometry. The electrochemical cell was formed by a three-electrode arrangement using Ag/AgCl as the reference electrode (KCl salt bridge), polymer coated on Pt disc as the working electrode and Pt foil as the counter electrode. In this manuscript, the sensing study of H_2O_2 was performed using PANI-SDS-P123 and PANI-SDS-BRIJ35 samples. For comparison, sensing was also performed using conventional PANI. The CV results show that PANI-SDS-P123 electrode on successive addition of H_2O_2 into 0.1 M phosphate buffer solution (PBS) (pH = 7.2) exhibits higher current than PANI for same concentration of H_2O_2 (Fig. 6a). Thus, PANI-SDS-P123 exhibits better electrocatalytic ability in the reduction and oxidation of H_2O_2 compared to PANI. In the case of PANI-SDS-BRIJ35, the CV depicts higher redox currents for H_2O_2 when compared with PANI. However, the redox currents are smaller when compared with PANI-SDS-P123. For example, the current response of 40 mM H_2O_2 at an operating potential of 0.6 V at PANI-SDS-P123, PANI-SDS-BRIJ35 and PANI modified electrodes were 88.8 μA, 67 μA, and 58.6 μA, respectively (Fig. 6b). CV results demonstrate that the sensing is far better using PANI-SDS-P123, hence continuous amperometry studies were performed using PANI-SDS-P123.

For continuous amperometry studies, aliquots of H_2O_2 solution were successively added to 0.1 M PBS (pH = 7.2) in which the three electrodes were dipped and the response was measured by

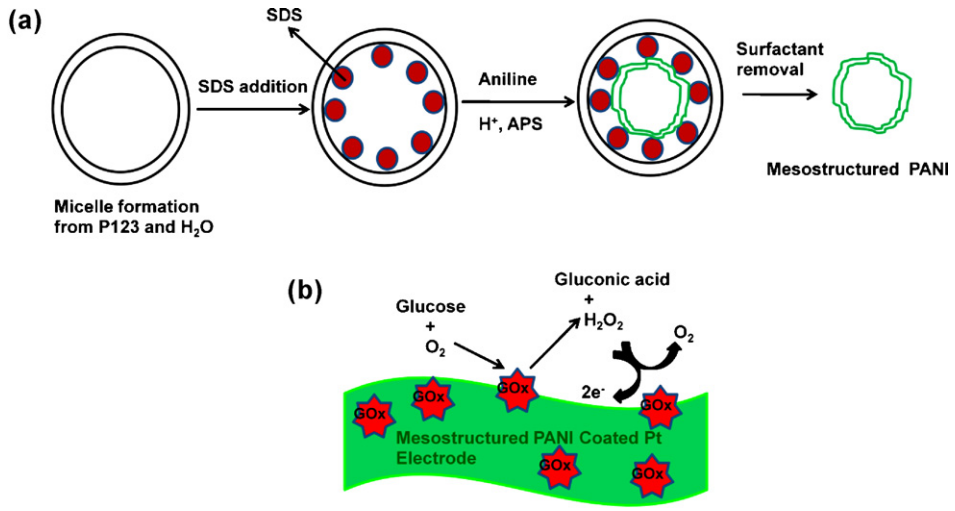

Scheme 1. (a) Schematic representation of the proposed mechanism for the formation of mesostructured PANI by the self-assembly of SDS and tri-block copolymer. (b) Modification of PANI-SDS-P123/PANI electrodes for efficient detection of glucose.

applying a potential of 0.4 V. Addition of each aliquot leads to increase in concentration by 2 mM. The amperometric current obtained is proportional to the concentration of H_2O_2 (Fig. 7a). PANI-SDS-P123 exhibits good sensitivity to H_2O_2 in a wide concentration range. The value of the current was plotted against the concentration of H_2O_2 to obtain a calibration plot (Fig. 7b). PANI-SDS-P123 exhibited higher sensitivity (2.27 μA/mM) when compared with PANI (0.77 μA/mM). PANI-SDS-P123 exhibits a linear dependence of the response current on the H_2O_2 concentrations in the range from 1 to 45 mM, whereas PANI showed linear response up to 20 mM indicating a less restricted diffusion of H_2O_2 through the porous PANI-SDS-P123 layer. The above CV and amperometry studies indicate that PANI-SDS-P123 has high sensing capability than PANI electrode due to its better permeability and electrocatalytic activity.

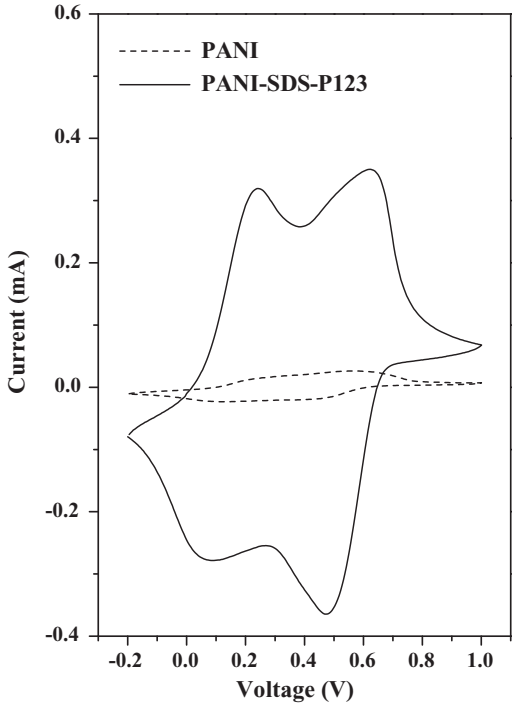

Fig. 5. Cyclic voltammograms of PANI-SDS-P123 and PANI in 1 M HCl.

3.3. Electrochemical sensing of glucose

The high electrocatalytic activity of PANI-SDS-P123 encouraged us to develop a glucose biosensor. For the preparation of the biosensor, glucose oxidase (GOx) was first encapsulated in

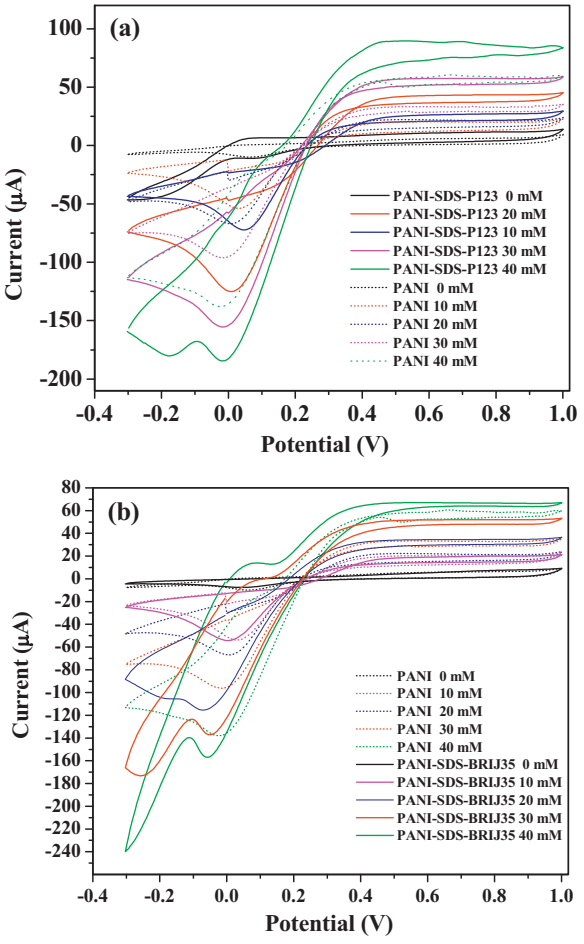

Fig. 6. Cyclic voltammograms of (a) PANI-SDS-P123 and PANI electrodes and (b) PANI-SDS-BRIJ35 and PANI electrodes, in the presence H_2O_2 in phosphate buffer solution (pH = 7.2) at a scan rate of 50 mV s^{-1}.

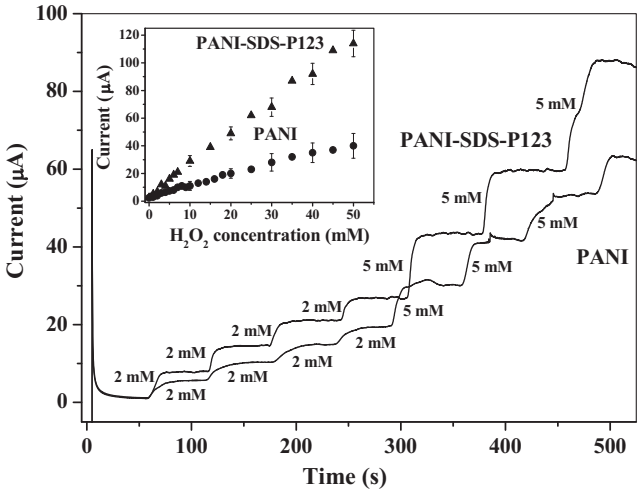

Fig. 7. Amperometric responses of the PANI-SDS-P123 and PANI electrodes to successive addition of H_2O_2. Inset shows the calibration curve for the biosensor response to H_2O_2.

the PANI-SDS-P123I/PANI. The working electrode for the glucose sensing is GOx entrapped PANI-SDS-P123 coated on Pt disc. Similar to H_2O_2 sensing, in this case also continuous amperometry was used to detect the amount of glucose. GOx enzyme immobilized on the PANI-SDS-P123 catalyzes the oxidation reaction of glucose to gluconic acid and hydrogen peroxide (Scheme 1b). Subsequently, H_2O_2 is oxidized causing an increase in current [via the reaction $H_2O_2 \rightarrow 2H^+ + O_2 + 2e^-$]. On the successive increase in glucose concentration, a significant increase in the response current was found, which indicates a good electrocatalytic performance and a fast electron exchange response of the PANI-SDS-P123/GOx electrode. Continuous amperometry method for the detection of glucose using PANI/GOx and PANI-SDS-P123/GOx confirms that the immobilized GOx is stable in the polymer matrix during these investigations (Fig. 8a). Calibration curve of PANI-SDS-P123/GOx clearly exhibits a linear dependence of the response current on the glucose concentration in the range from 1 to 20 mM, whereas PANI/GOx showed the linear response up to 10 mM (Fig. 8b), which shows PANI-SDS-P123/GOx has high sensing capability than PANI/GOx electrode.

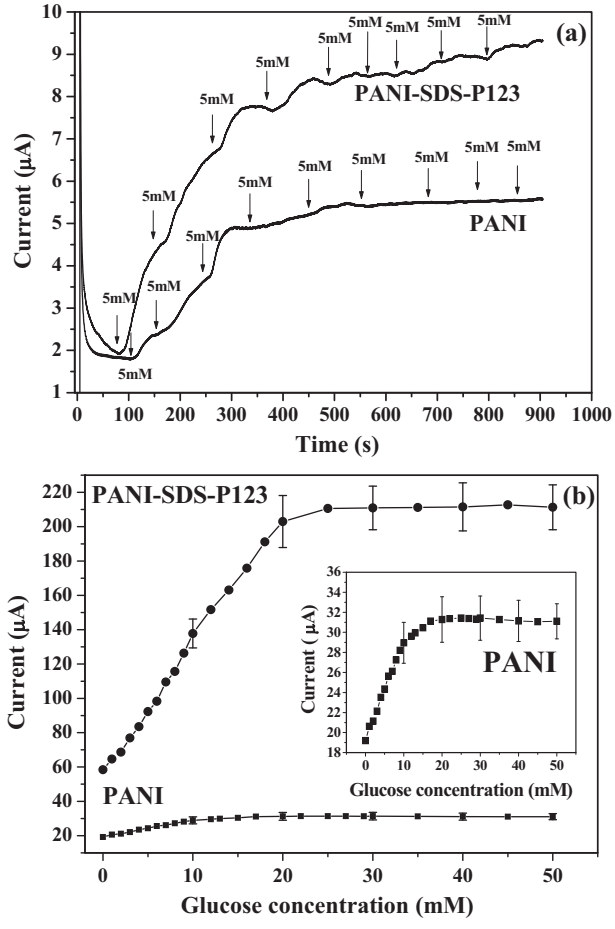

Fig. 8. (a) Amperometric responses of the PANI-SDS-P123/GOx and PANI/GOx electrodes to successive addition of glucose and (b) Calibration curve for the biosensor response to glucose; Inset: magnified plot for the response of PANI/GOx electrodes to glucose.

4. Conclusions

The study has demonstrated an efficient and simple route to synthesize mesostructured PANI by the self-assembly of mixed (ionic and non-ionic) soft template methodology, followed by its application in the sensing of H_2O_2 and glucose. PANI-SDS-P123/GOx exhibited higher sensitivity (2.27 μA/mM) when compared with PANI (0.77 μA/mM) in H_2O_2 sensing. Glucose sensing studies clearly show that PANI-SDS-P123/GOx exhibits a linear dependence of the response current on the glucose concentration in the range from 1 to 20 mM, whereas PANI/GOx showed the linear response up to 10 mM, which shows that PANI-SDS-P123/GOx has high sensing capability than PANI/GOx electrode. Because of the large specific surface area, excellent conductivity and high porosity, PANI-SDS-P123/GOx easily provides larger effective surface area to immobilize GOx. Moreover, the nanoporous PANI-SDS-P123/GOx allows the rapid electron-transfer and hence enhance the glucose-response. Although the concept has been presented within the context of glucose-sensing, it could be readily extended to other bio-catalytic systems based on the ample selection of enzymes.

Acknowledgments

Authors thank Council of Scientific and Industrial Research, New Delhi for financial assistance. Authors also thank Prof. M. K. Surappa, Director, IIT Ropar for his encouragement.

References

[1] Y. Meng, D. Gu, F. Zhang, Y. Shi, H. Yang, Z. Li, C. Yu, B. Tu, D. Zhao, Angew. Chem. Int. Ed. 44 (2005) 7053.
[2] A.G. MacDiarmid, Synth. Met. 125 (2001) 11.
[3] S. Holdcroft, Adv. Mater. 13 (2001) 1753.
[4] J. Liu, S. Tian, W. Knoll, Langmuir 21 (2005) 5596.
[5] J. Yang, S.M. Burkinshaw, J. Zhou, A.P. Monkman, P.J. Brown, Adv. Mater. 15 (2003) 1081.
[6] C.G. Wu, T. Bein, Science 264 (1994) 1757.
[7] A.P. Alivisatos, Science 271 (1996) 933.
[8] J. Janata, M. Josowicz, Nat. Matters 2 (2003) 19.
[9] H.J. Choi, M.S. Jhon, Soft Matter 5 (2009) 1562.
[10] S. Sukeerthi, A.Q. Contractor, Anal. Chem. 71 (1999) 2231.
[11] J. Lu, B.J. Park, B. Kumar, M. Castro, H.J. Choi, J.-F. Feller, Nanotechnology 21 (2010) 10, 255501.
[12] A. Baba, W. Knoll, Adv. Mater. 15 (2003) 1015.
[13] X. Zhang, W.J. Goux, S.K. Manohar, J. Am. Chem. Soc. 126 (2004) 4502.
[14] C.R. Martin, Chem. Mater. 8 (1996) 1739.
[15] J.C. Michaelson, A.J. McEvoy, Chem. Commun. 79 (1994).
[16] Z.X. Wei, Z.M. Zhang, M.X. Wan, Langmuir 18 (2002) 917.
[17] J. Huang, R.B. Kaner, J. Am. Chem. Soc. 126 (2004) 851.
[18] I.D. Norris, M.M. Shaker, F.K. Ko, A.G. Macdiarmid, Synth. Met. 114 (2000) 109.
[19] X.L. Jing, Y.Y. Wang, D. Wu, L. She, Y. Guo, J. Polym. Sci. A: Polym. Chem. 44 (2006) 1014.
[20] H. Qiu, M. Wan, B. Matthews, L. Dai, Macromolecules 34 (2001) 675.
[21] D. Zhang, Y. Wang, Mater. Sci. Eng. A 134 (2006) 9.
[22] L. Liang, J. Liu, C.F. Windisch, G.J. Exarhas Jr., Y. Lin, Angew. Chem. Int. Ed. 41 (2002) 3665.

[23] A.G. MacDiarmid, W.E. Jones Jr., I.D. Norris, J. Gao, A.T. Johnson, N.J. Pinto, J. Hone, B. Han, F.K. Ko, H. Okuzaki, M. Llaguno, Synth. Met. 119 (2001) 27.
[24] H.X. He, C.Z. Li, N.J. Tao, Appl. Phys. Lett. 78 (2001) 811.
[25] C.W. Wang, Z. Wang, M.K. Li, H.L. Li, Chem. Phys. Lett. 341 (2001) 431.
[26] H. Cao, C. Tie, Z. Xu, J. Hong, H. Sang, Appl. Phys. Lett. 78 (2001) 1592.
[27] X. Zhang, R.C.Y. King, A. Jose, S.K. Manohara, Synth. Met. 145 (2004) 23.
[28] H. Sangodkar, S. Sukeerthi, R.S. Srinivasa, R. Lal, A.Q. Contractor, Anal. Chem. 68 (1996) 779.
[29] P.K. Prabhakar, S. Raj, P.R. Anuradha, S.N. Sawant, M. Doble, Colloids Surf. B Biointerfaces 86 (2011) 146.
[30] D. Lu, T. Katou, M. Uchida, J.N. Kondo, K. Domen, Chem. Mater. 17 (2005) 632.
[31] N. Gospodinova, P. Mokreva, T. Tsanov, L. Terlemezyan, Polymer 38 (1997) 743.
[32] S.R. Lee, Y.T. Lee, K. Sawada, H. Takao, M. Ishida, Biosens. Bioelectron. 24 (2008) 410.
[33] J.D. Newman, A.P.F. Turner, Biosens. Bioelectron. 20 (2005) 2435.
[34] L. Wu, X. Zhang, H. Ju, Biosens. Bioelectron. 19 (2007) 1461.
[35] R.R. Banerjee, S.M. Rangwala, J.S. Shapiro, A.S. Rich, B. Rhoades, Y. Qi, J. Wang, M.W. Rajala, A. Pocai, P.E. Scherer, C.M. Steppan, R.S. Ahima, S. Obici, L. Rossetti, M.A. Lazar, Science 303 (2004) 1195.
[36] Z.Y. Wang, X.N. Liu, P. Wu, C.X. Cai, Anal. Chem. 81 (2009) 1638.
[37] Q. Xua, C. Mao, N.N. Liu, J.J. Zhu, J. Sheng, Biosens. Bioelectron. 22 (2006) 768.
[38] Y. Xiao, F. Patolsky, E. Katz, J.F. Hainfeld, I. Willner, Science 299 (2003) 1877.
[39] J. Jia, B. Wang, A. Wu, G. Cheng, Z. Li, S.A. Dong, Anal. Chem. 74 (2002) 2217.
[40] S. Palaniappan, A. John, C. Amarnath, V. Rao, J. Mol. Catal. A: Chem. 218 (2004) 47.
[41] Z.M. Zhang, Z.X. Wei, M.X. Wan, Macromolecules 35 (2002) 5937.
[42] K.H. Lee, D.H. Song, B.J. Park, I.J. Chin, H.J. Choi, Macromol. Theory Simul. 18 (2009) 287.
[43] K. Huang, M.X. Wan, Chem. Mater. 14 (2002) 3486.
[44] P.A. McCarthy, J. Huang, S.C. Yang, H.L. Wang, Langmuir 18 (2002) 259.
[45] H. Liu, X.B. Hu, J.Y. Wang, R.I. Boughton, Macromolecules 35 (2002) 9414.
[46] C. Bian, A. Yu, Synth. Met. 160 (2010) 1579.
[47] J. Huang, S. Virji, B.H. Weiller, R.B. Kaner, J. Am. Chem. Soc. 125 (2003) 314.
[48] W. Zhao, L. Ma, K. Lu, J. Polym. Res. 14 (2007) 1.
[49] P. Wang, K.L. Tan, E.T. Kang, K.G. Neoh, Appl. Surf. Sci. 193 (2002) 36.
[50] M.R. Nabid, R. Sedghi, P.R. Jamaat, N. Safari, A.A. Entezami, J. Appl. Polym. Sci. 102 (2006) 2929.
[51] E.N. Konyushenko, S. Reynaud, V. Pellerin, M. Trchová, J. Stejskal, I. Sapurina, Polymer 52 (2011) 1900.
[52] K. Shah, J. Iroh, Synth. Met. 132 (2002) 35.
[53] D. Zhao, J. Feng, Q. Huo, N. Melosh, G.H. Fredrickson, B.F. Chmelka, G.D. Stucky, Science 279 (1998) 548.
[54] M.U. Anu Prathap, R. Srivastava, J. Colloid Interface Sci. 358 (2011) 399.